Spherical t-Design for Characterizing the Spatial Response of Microphone Arrays

Daniel Pinardi
Dept. of Engineering and Architecture
University of Parma
Parma, Italy
daniel.pinardi@unipr.it

2021 Immersive and 3D Audio: from Architecture to Automotive (I3DA) | 978-1-6654-0998-8/21/$31.00 ©2021 IEEE | DOI: 10.1109/I3DA48870.2021.9610850

***Abstract*—Microphone arrays are usually employed for spatial audio recordings and analysis. This requires converting the raw signals of the capsules into a 3D audio format, e.g., a spherical harmonics expansion. For processing such conversion, namely beamforming, it is necessary to know the complex response of each microphone of the array for many Directions-of-Arrival of the sound waves. This information constitutes the spatial response and describes how the wave fronts are diffracted by the surface of the array. Beyond the experimental, numerical, or theoretical method employed to get the spatial response, the shape of the array and the number of capsules, the choice of the Directions-of-Arrival of the sound waves is always critical. On one side, to maximize the spatial information and so the performance, on the other side to reduce the number of directions, and so the measurement or calculation time. The paper analyzes the problem of choosing an optimal geometry for obtaining the spatial response of a microphone array. It will be shown that spherical design, or T-design, allows maximizing the spatial information with the minimum amount of testing directions. Numerical and theoretical methods have been employed for characterizing two microphone arrays, a spherical and a non-spherical one. In both cases, Ambisonics format for spatial audio has been employed.**

Keywords— Ambisonics, beamforming, microphone array, spatial audio, spherical design, T-design

I. Introduction

Microphone arrays are widely employed for recording the sound field while preserving the directional information. This can be obtained, for instance, with a spherical harmonic (SH) [1] expansion of the signals recorded by the capsules of the microphone array, as it happens for the Ambisonics theory [2]. Such conversion can be done through linear [3] or parametric processing [4], [5], [6], [7], [8], [9]. In the first case, a matrix of filters is employed, while in the second case a spatial analysis of the sound scene is performed first, extracting the source signals and their locations, and then theoretical SH formulas are used.

Regardless the beamforming method, the complex response of each capsule of the microphone array for many Directions-of-Arrival (DoA) of the sound waves is required. Such result can be obtained with three approaches: experimental, numerical, and theoretical. The experimental method consists in measuring the microphone array in an anechoic chamber [10], either rotating the microphone array or employing a moving loudspeaker. The theoretical method relies on the analytical equations that describe the interaction between the sound waves and the geometry of the microphone array [11], [12], [13]. Finally, the numerical approach solves the diffraction problem with simulations, typically Finite Elements Method (FEM) or Boundary Elements Method (BEM) [14], [15], [16]. In each of these cases, a grid of DoA must be employed for testing the array, and therefore the problem of making the most efficient choice arises, with the aim of reducing the measurement or calculation time without loss of information.

In this paper, it will be shown that the spherical designs, or T-designs, [17], [18] are the optimal geometries for calculating the complex response of microphone arrays with sound waves arriving from many DoA. The numerical and theoretical approaches were used to calculate the diffraction of plane waves, employing three different types of grids: equiangular, nearly uniform, and spherical designs. Two arrays were studied: one is equipped with four capsules arranged over a sphere having 30 mm diameter, the second one is a non-spherical array with 32 capsules. The Ambisonics format has been encoded through a matrix of Finite Impulse Response (FIR) filters, calculated with a regularized Kirkeby inversion [19], [20], [21], using first order Ambisonics (FOA) for the spherical array with four capsules, and high order Ambisonics (HOA) up to order four for the non-spherical array with 32 capsules. Three parameters, Spatial Correlation (SC), Level Difference (LD), and White Noise Gain (WNG) [22], [23] were used for assessing the spatial performance, thus allowing to compare the DoA.

The paper is organized as follow. Section II describes the beamforming algorithm and the evaluation metrics. Section III provides the theoretical basis of the spherical designs. In section IV the various geometries analyzed are presented. Section V and section VI show the results and, finally, section VII summarizes the conclusions.

II. Ambisonics Format, Encoding and Evaluation

A linear processing has been used for encoding the Ambisonics format, leaving parametric methods to future development. The beamforming matrix of FIR filters is computed in frequency domain by means of the regularized Kirkeby inversion:

$$H_{m,v,k} = \left[C^*_{m,d,k} \cdot C_{m,d,k} + \beta_k \cdot I\right]^{-1} \cdot \left[C^*_{m,d,k} \cdot A_{d,v} \cdot e^{-j\pi k}\right] \quad (1)$$

where $m = [1, \dots, M]$ are the capsules; $v = [1, \dots, V]$ are the virtual microphones; k is the frequency index; $d = [1, \dots, D]$ are the DoA of the sound waves; the matrix C is the complex response of each capsule m for each direction d; the matrix A defines the frequency independent amplitude of the target directivity patterns; $e^{-j\pi k}$ introduces a latency that ensures filters causality; $\cdot$ is the dot product; I is the identity matrix; $[\,]^*$ denotes the conjugate transpose; $[\,]^{-1}$ denotes the pseudo-inverse; β is a frequency-dependent regularization parameter [21].

In this work, Ambisonics format is employed, therefore the coefficients of the target directivity matrix A are those of the SH functions, usually defined as follows [24]:

$$A_{d,v} = \sqrt{\frac{(2n+1)}{4\pi}\frac{(n-v)!}{(n+v)!}}\, P_n^v(\cos\theta) e^{iv\varphi} \quad (2)$$

where (θ, φ) are the angles of each direction d, respectively elevation and azimuth; n is the degree of the SH, an integer value ≥ 0; v is the order of the SH, comprised in the range $[-n \leq v \leq +n]$; P_n^v are the associated Legendre polynomials [24]. The Ambisonics format employed in this work is compliant with the current standard *AmbiX* [25], which defines SN3D amplitude scaling and ACN numbering. The explicit formulas of SH to be used in (1) to define the target directivity A can be found in [26], up to order five.

The matrix H is converted back to time domain by means of the Inverse Fast Fourier Transform (IFFT), thus obtaining the matrix h, having dimensions [M;V;N], where N is the number of samples of each FIR filter. The effective directivity A' for each virtual microphone v in each direction d is obtained, in frequency domain, as follows:

$$A'_{d,v,k} = \sum_{m=1}^{M} C_{m,d,k} \cdot H_{m,v,k} \tag{3}$$

where $d = [1, \dots, D]$ and $k = [1, \dots, N/2]$. Ideally, i.e., in case of perfect reconstruction, the matrix A' would be frequency independent, thus resulting in $A' = A$ for all the d directions at all frequencies.

The SC and LD metrics, employed for assessing the spatial performance obtained with different DoA grids, are defined as:

$$SC_{v,k} = \frac{\sum_{d=1}^{D} (A'_{d,v,k})^T \cdot A_{d,v}}{\sum_{d=1}^{D}\left(\sqrt{(A'_{d,v,k})^T \cdot A'_{d,v,k}} \cdot \sqrt{(A_{d,v})^T \cdot A_{d,v}}\right)} \tag{4}$$

$$LD_{v,k} = \frac{1}{D} \sum_{d=1}^{D} \frac{(A_{d,v})^2}{A'_{d,v,k} \cdot (A'_{d,v,k})^*} \tag{5}$$

where $[\,]^T$ denotes the transpose. Both metrics are averaged over the virtual microphones of order v belonging to the degree n:

$$SC_{n,k} = \frac{1}{2n+1} \sum_{v=-n}^{n} \left| SC_{v,k} \right| \tag{6}$$

$$LD_{n,k} = -10 \log \left[\frac{1}{2n+1} \sum_{v=-n}^{n} LD_{v,k} \right] \tag{7}$$

SC varies in the range $0 \div 1$, while LD varies in the range $-\infty \div +\infty \, [dB]$. Each Ambisonics order is perfectly reconstructed if:

$$SC_{ideal} = 1 \tag{8}$$

$$LD_{ideal} = 0 \, [dB] \tag{9}$$

However, a certain amount of error can be accepted. Therefore, in this work the following two ranges of acceptability are employed:

$$SC_{acc.range} = [0.95; 1] \tag{10}$$

$$LD_{acc.range} = [-1; +1] \, [dB] \tag{11}$$

Frequency limits for each order are found considering the most restricted combination provided by the two parameters.

Finally, the amplification of the SH is evaluated through the maximum eigenvalues of the filtering matrix H for all SH and directions at each frequency. Usually, this is known as White Noise Gain (WNG):

$$WNG_k = \max_k [\lambda(H_k^* \cdot H_k)] \tag{12}$$

where λ denotes the eigenvalues. WNG should be as low as possible at all frequencies.

III. Spherical Design theory

Spherical t-designs have been introduced in [17], where the authors proposed to approximate a unit sphere in $\mathbb{R}_n$ with a finite set of points (called a spherical t-design) so that the integral over the sphere of a polynomial of degree t (or less) is equal to the average value of the same polynomial evaluated in the t-design set of points. In other words, spherical t-designs provide equal weight quadrature rules on a sphere. Hence, in $\mathbb{R}_3$ a set of P points $p = [J_1, \dots, J_P]$ on a unit sphere S is a spherical t-design if, for any polynomial f of degree at most t, it is satisfied:

$$\int_S f(x) \cdot dS = \frac{1}{P} \cdot \sum_{i=1}^{P} f(J_i) \tag{13}$$

Therefore, given a certain value of P points, the aim is to choose their positions to maximize t. This means that such an optimal choice of the positions of these points ensures to be able to capture the spatial information up to a maximally high spatial frequency.

Generally, the spherical t-designs are not unique, although some very rare cases were found to be rigid [27]. The rigid designs are unique for given t and P up to an orthogonal transformation. Another important definition is a tight spherical t-design, meaning it has a minimum cardinality [17]. Tight designs are also rigid designs [28], meaning they are unique and have the best combinatorial properties at the same time. For the case of $\mathbb{R}_3$, only the following rigid tight designs were identified:
1-design that consists of 2 antipodal points.
2-design that consists of 4 points (a tetrahedron).
3-design that consists of 6 points (an octahedron).
5-design that consists of 12 points (an icosahedron).

Large t-designs that exceed the Platonic solids are mostly computed numerically instead of being constructed in explicit analytical manner. More on existence and construction of spherical t-designs can be found in [29], [30], [31], [32]. However, the techniques used to compute t-designs are beyond the scope of this paper. Many of the sets were computed, and made publicly available: in [18], the solutions for P ranging between 1 and 100 are found showing that, despite a general trend of P increasing with t, some solutions exhibit a large value of t with a relatively small value of P. It is interesting to note that these remarkable geometries do not correspond to known Archimedean solids, being instead the result of a numerical optimization, such as the Archimedean snub cube, which has 24 vertices and is only a 3-design. Neither they belong to rigid t-designs, meaning the disposition of points for each of them is not unique.

Furthermore, it appears that all possible t-design geometries up to (*P=240, t=21*) have been already found, and some have been found reaching (*P=100200, t=1000*) [33]. Therefore, the already found t-design geometries are employed in this work. It must be noted that the number of points P of the spherical designs corresponds here to the number D of DoA of the sound waves. Some applications of t-design geometries to microphone arrays design can be found in [34], [35].

IV. Test Geometries for Microphone arrays

As described in the introduction of this work, three kinds of grids have been compared: equiangular, nearly uniform, and spherical design. Two different sizes for each type were used, one with fewer points for the FOA case and one with more points for the HOA case.

The equiangular grid is obtained with a constant spacing δ for both azimuth and elevation, respectively: $\delta = 20°, D = 171$ (Fig. 1) and $\delta = 12°, D = 465$ (Fig. 2).

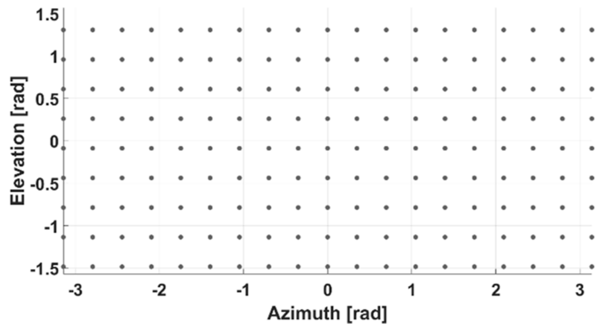

Fig. 1. Equiangular grid, $\delta = 20°, D = 171$.

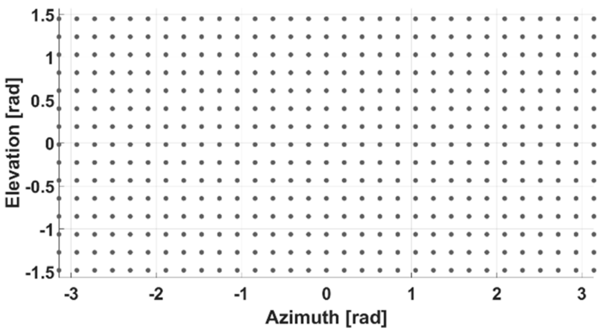

Fig. 2. Equiangular grid, $\delta = 12°, D = 465$.

The nearly uniform grid, called "balloon" in the following, is obtained by subdividing sequentially a sphere into triangles for a certain number of times τ, starting from the vertexes of a dodecahedron (Fig. 3). The two configurations are: $\tau = 4, D = 122$ (Fig. 4) and $\tau = 6, D = 362$ (Fig. 5).

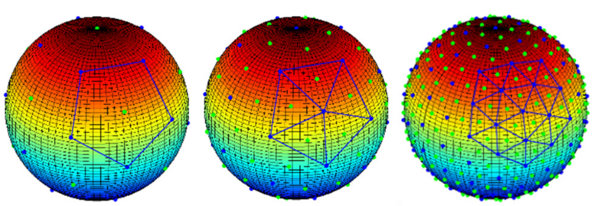

Fig. 3. Nearly uniform subdivision of a sphere into triangles.

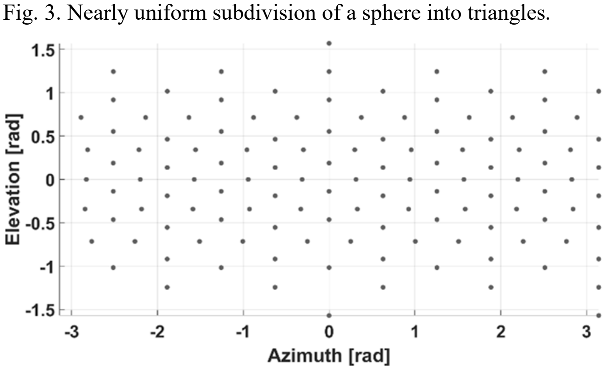

Fig. 4. Nearly uniform grid, $\tau = 4, D = 122$.

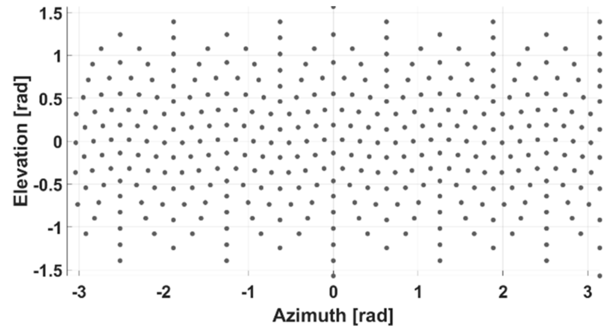

Fig. 5. Nearly uniform grid, $\tau = 4, D = 362$.

Finally, many spherical designs of various orders were tested, with the aim of optimizing the spatial performance while reducing the number of directions. The two optimal configurations presented here are: $T = 10$, $D = 60$ (Fig. 6) and $T = 21, D = 240$ (Fig. 7).

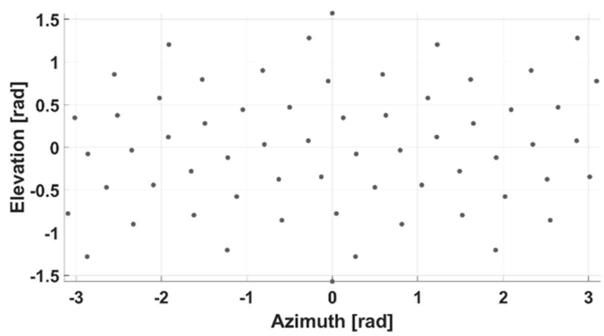

Fig. 6. Spherical design, $T = 10, D = 60$.

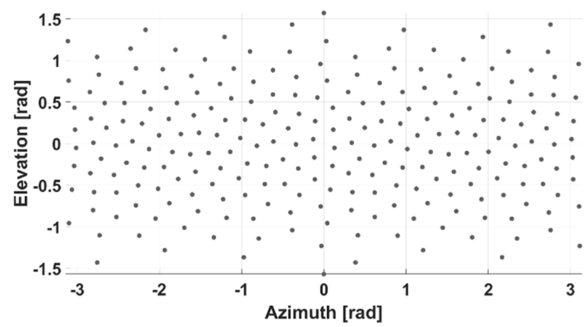

Fig. 7. Spherical design, $T = 21, D = 240$.

V. First Order Ambisonics Microphone Array

The theoretical method was employed for studying a FOA (*n=0;1*) spherical microphone array of 15 mm radius and provided with four capsules, arranged in the vertices of a tetrahedron. The first analytical solution of the equations describing the plane wave diffraction over a rigid sphere was discussed in [36]. The solution was further generalized and simplified for practical applications, thus, evolving in what is commonly used in microphone array processing [37]. The total pressure on a spherical surface encountered by a plane wave is defined by:

$$P_{\text{tot}}(R, \theta, \phi) = \frac{4\pi i}{(kR)^2} \sum_{n=0}^{\infty} \frac{i^n}{h_n'(kR)} \sum_{m=-n}^{n} Y_n^m(\theta, \phi) Y_n^m(\vartheta, \varphi)^* \quad (14)$$

where R is the sphere radius (15 mm); k is the wave number; $h_n()$ is the spherical Hankel function; $()'$ denotes a derivative; $()^*$ denotes a complex conjugate; the angles φ and ϑ define the incident plane wave for each direction d.

Thus, in any point of the sphere and for any incident wave direction the complex sound pressure can be computed. An implementation of the described methodology can be found in [38].

The spatial response of this model was calculated employing the following three grids: equiangular ($\delta = 20°, D = 171$, Fig. 1), balloon ($\tau = 4, D = 122$, Fig. 4), and spherical design ($T = 10$, $D = 60$, Fig. 6). Comparative results of the three grids are shown in Fig. 8, Fig. 9, and Fig. 10 for SC metric and in Fig. 11, Fig. 12, and Fig. 13 for LD metric. WNG metric is shown in Fig. 14. One can note that LD is identical for the three cases. Instead, SC is worsened at low frequencies for the equiangular grid and identical for the others, despite the balloon has almost three times the number of directions of the spherical design. Finally, the WNG provided by the spherical design grid is the lowest of the three cases. Therefore, the spherical design ($T = 10, D = 60$) resulted the optimal choice for testing a FOA microphone array.

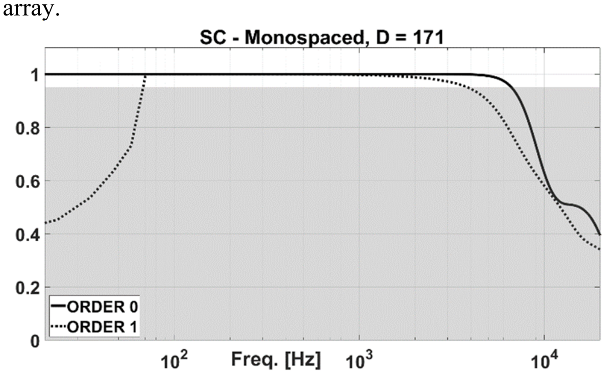

Fig. 8. FOA microphone array, theoretical method, SC metric, equiangular grid ($\delta = 20°, D = 171$).

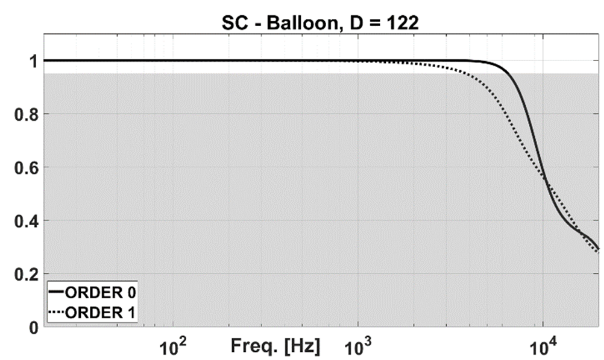

Fig. 9. FOA microphone array, theoretical method, SC metric, balloon grid ($\tau = 4, D = 122$)

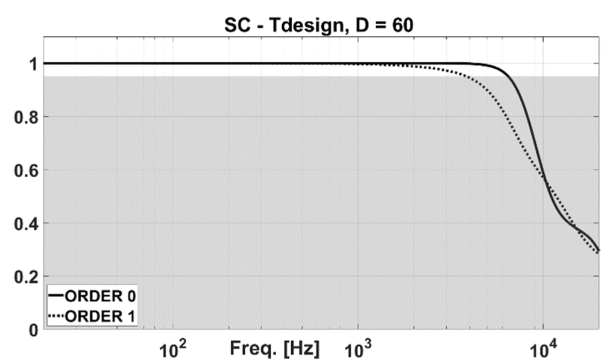

Fig. 10. FOA microphone array, theoretical method, SC metric, spherical design grid ($T = 10, D = 60$).

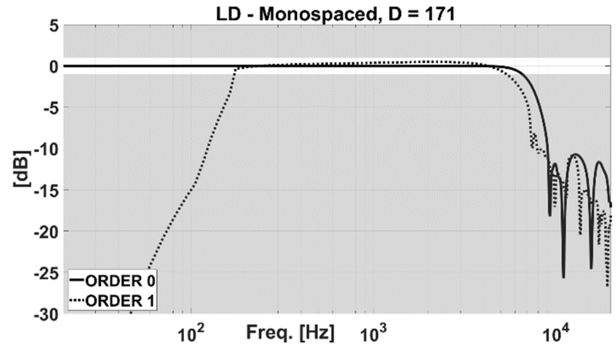

Fig. 11. FOA microphone array, theoretical method, LD metric, equiangular grid ($\delta = 20°, D = 171$).

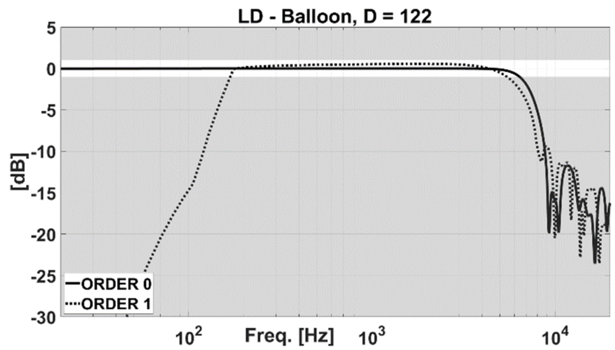

Fig. 12. FOA microphone array, theoretical method, LD metric, balloon grid ($\tau = 4, D = 122$).

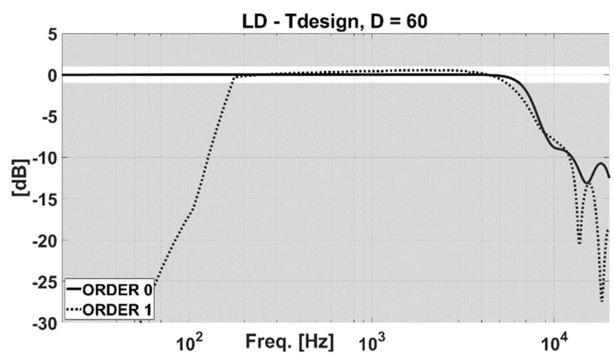

Fig. 13. FOA microphone array, theoretical method, LD metric, spherical design grid ($T = 10, D = 60$).

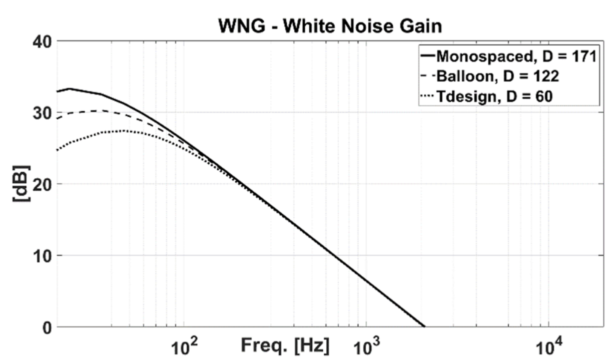

Fig. 14. FOA microphone array, theoretical method, WNG metric, comparison of the three grids.

VI. High Order Ambisonics Microphone Array

The numerical method solves the diffraction problem in a simulation. Not being constrained by the analytical equations, the approach is suitable for arrays of any geometry. A FEM simulation was calculated in COMSOL Multiphysics for a non-spherical array (Fig. 15) provided with 32 capsules, therefore capable to encode HOA. Ambisonics format was calculated up to order four. The simulation was solved in the frequency range $20\,Hz - 3.5\,kHz$, with a resolution of $10\,Hz$, and employing the plane wave radiation. More details are available in [39].

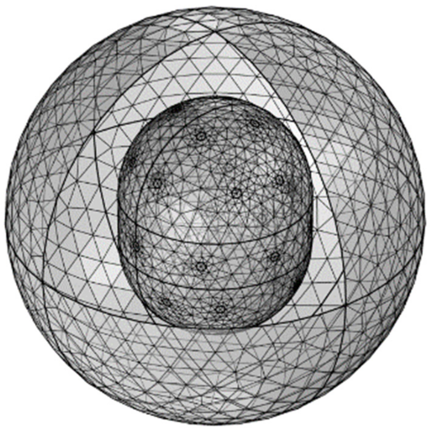

Fig. 15. FEM model of a non-spherical microphone array.

The simulation was repeated employing different DoA grids. Results are presented here for the following three configurations: equiangular ($\delta = 12°, D = 465$, Fig. 2), balloon ($\tau = 6, D = 362$, Fig. 5), and spherical design ($T = 21, D = 240$, Fig. 7). Comparative results of the three grids are shown in Fig. 16, Fig. 17, and Fig. 18 for SC metric and in Fig. 19, Fig. 20, and Fig. 21 for LD metric. Ambisonics orders *n=1;2;3;4* are shown (*n=0* is omitted for improving plot readability). WNG metric is shown in Fig. 22. One can note that also in this case the LD is very similar among the three cases, while SC is slightly worsened at low frequency with the equiangular grid and almost identical with the others. The WNG metric is clearly lower employing the spherical design. Therefore, the spherical design ($T = 21, D = 240$) resulted the optimal geometry for testing a HOA microphone array up to fourth order.

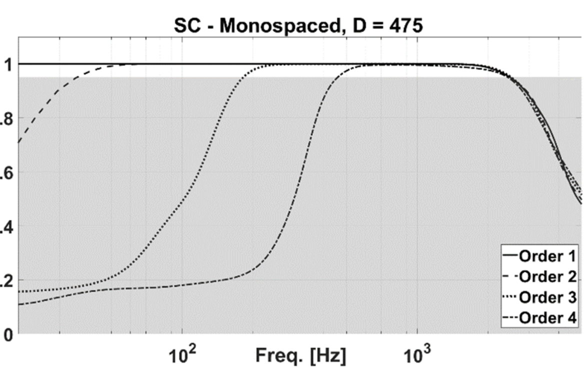

Fig. 16. HOA microphone array, numerical method, SC metric, equiangular grid ($\delta = 12°, D = 465$).

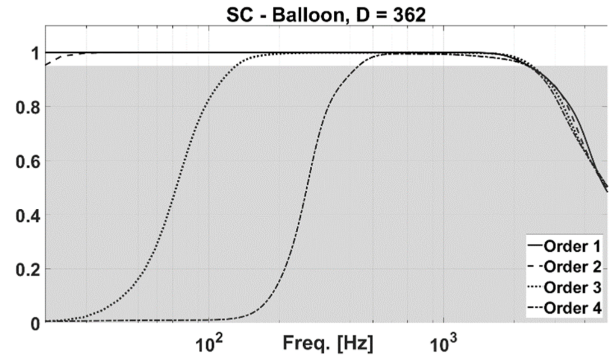

Fig. 17. HOA microphone array, numerical method, SC metric, balloon grid ($\tau = 6, D = 362$).

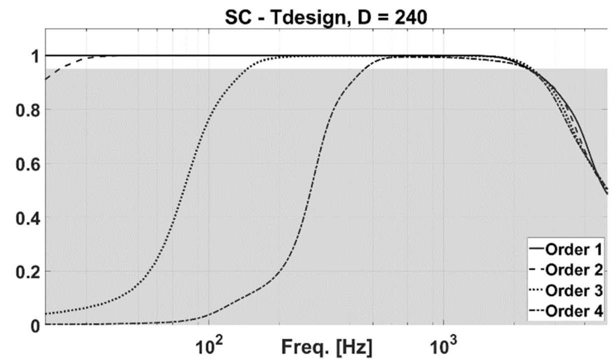

Fig. 18. HOA microphone array, numerical method, SC metric, spherical design grid ($T = 21, D = 240$).

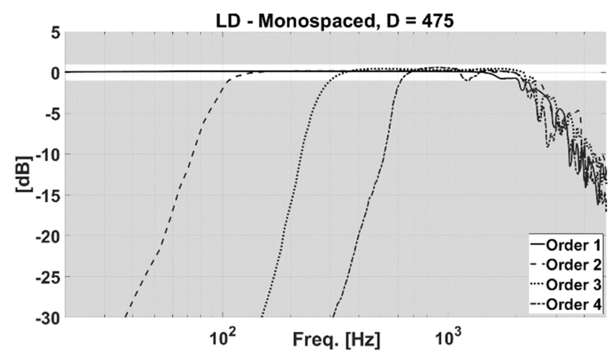

Fig. 19. HOA microphone array, numerical method, LD metric, equiangular grid ($\delta = 12°, D = 465$).

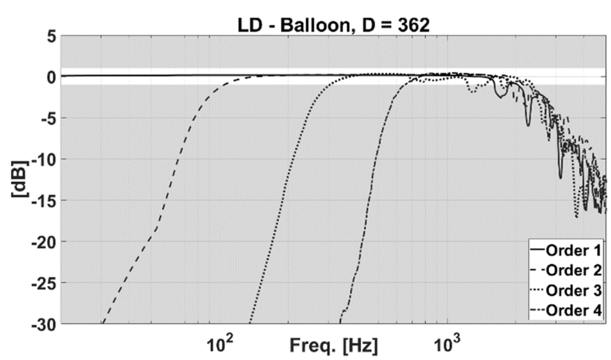

Fig. 20. HOA microphone array, numerical method, LD metric, balloon grid ($\tau = 6, D = 362$).

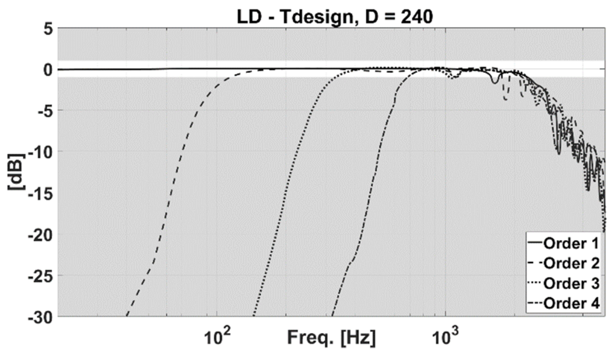

Fig. 21. HOA microphone array, numerical method, LD metric, spherical design grid ($T = 21, D = 240$).

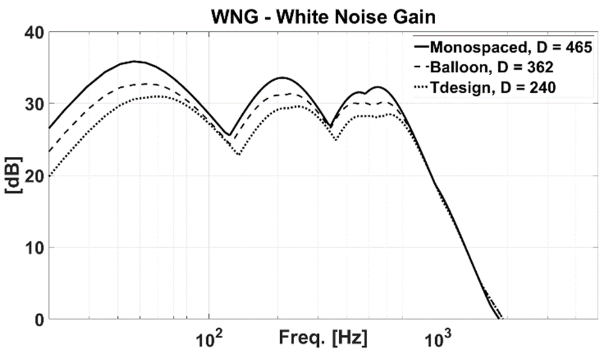

Fig. 22. HOA microphone array, numerical method, WNG metric, comparison of the three grids.

VII. Conclusions

Several distributions of points for characterizing the complex response of the capsules of microphone arrays for many Directions-of-Arrival of the sound waves were evaluated: equiangular, nearly uniform, and spherical design. The purpose of the study is to find optimal testing grids, for maximizing the spatial response with the minimum number of directions.

Two microphone arrays have been studied, having spherical and non-spherical shape, and using the theoretical and the numerical method respectively, to solve the diffraction of plane waves over the surface of the arrays. Then, Ambisonics spatial audio format was calculated up to order one for the FOA case (spherical array with four capsules) and up to order four for the HOA case (non-spherical array with 32 capsules). The spatial performance of each array was evaluated with three metrics, namely Spatial Correlation, Level Difference and White Noise Gain, allowing to compare the results provided by the different grids of DoA employed to get the microphone arrays responses.

Spherical t-designs revealed to be the most efficient geometries for obtaining the complex response of the capsules of microphone arrays, since they allow to maximize the spatial performance with the minimum number of DoA to test. The spherical design of order $T = 10$ having $D = 60$ points resulted the optimal geometry for First Order Ambisonics microphone array. Instead, a spherical design of order $T = 21$ having $D = 240$ points resulted the optimal geometry for a microphone array capable to operate up to Ambisonics fourth order.

References

[1] N. M. Ferres, "An Elementary Treatise on Spherical Harmonics and Subjects Connected with them," *London: Macmillan and Co.,* 1877.

[2] M. A. Gerzon, "Periphony: With-height Sound Reproduction," *Journal of the Audio Engineering Society,* vol. 21, pp. 2-10, 1973.

[3] A. Farina, S. Campanini, L. Chiesi, A. Amendola and L. Ebri, "Spatial Sound Recording With Dense Microphone Arrays," *55th AES Conference,* August 2014.

[4] RODE Microphones, «Soundfield plug-in,» 2018. [Online]. Available: https://it.rode.com/soundfieldplugin.

[5] S. Delikaris-Manias and V. Pulkki, "Parametric Spatial Filter Utilizing Dual Beamformer and SNR-Based Smoothing," in *AES 55th International Conference: Spatial Audio*, 2014.

[6] V. Pulkki, "Directional audio coding in spatial sound reproduction and stereo upmixing," in *Proc. 28th AES International Conference*, Pitea, 2006.

[7] V. Pulkki, "Spatial Sound Reproduction with Directinal Audio Coding," *Journal of the AES,* vol. 55, no. 6, pp. 503-516, 2007.

[8] S. Berge and N. Barrett, "High Angular Resolution Planewave Expansion (HARPEX)," in *Proc. of the 2nd International Symposium on Ambisonics and Spherical Acoustics*, 2010.

[9] V. Pulkki, A. Politis, M. V. Laitinen, J. Vilkamo and J. Ahonen, "First-order directional audio coding (DirAC)," in *Parametric Time-Frequency Domain Spatial Audio*, 2017, pp. 89-138.

[10] A. Farina, A. Capra, L. Chiesi and L. Scopece, "A Spherical Microphone Array for Synthesizing Virtual Directive Microphones in Live Broadcasting and in Post Production," *40th International Conference: Spatial Audio: Sense the Sound of Space,* 2010.

[11] L. McCormack, S. Delikaris-Manias, A. Farina, D. Pinardi and V. Pulkki, "Real-time conversion of sensor array signals into spherical harmonic signals with applications to spatially localised sub-band sound-field analysis," *144th AES Convention,* 2018.

[12] Institute of Electronic Music and Acoustics, "IEM Plug-in Suite," [Online]. Available: https://plugins.iem.at/download/.

[13] L. McCormack, S. Delikaris-Manias, A. Politis, D. Pavlidi, A. Farina, D. Pinardi and V. Pulkki, "Applications of spatially localized active-intensity vectors for sound-field visualization," *Journal of the Audio Engineering Society,* vol. 67, no. 11, pp. 840-854, 2019.

[14] F. Kaiser, F. Zotter and H. Pomberger, "Investigations on cylindrical microphone arrays," in *25th AES UK Conference*, York, 2012.

[15] J. Daniel and N. Epain, "Improving Spherical Microphone Arrays," in *124th AES Convention*, Amsterdam, 2008.

[16] K. Tontiwattanakul, "Signal processing for microphone arrays with novel geometrical design," University of Southampton, Faculty of Engineering and the Environment, Southampton, 2016.

[17] P. Delsarte, J. M. Goethals and J. J. Seidel, “Spherical codes and designs,” *Geometriae Dedicata,* vol. 6, pp. 363-388, 1977.

[18] R. H. Hardin and N. J. A. Sloane, "McLaren's Improved Snub Cube and Other New Spherical Designs in Three Dimensions," *Discrete and Computational Geometry,* vol. 15, pp. 429-441, 1996.

[19] O. Kirkeby and P. A. Nelson, "Digital Filter Design for Inversion Problems in Sound Reproduction," *Journal of Audio Engineering Society,* vol. 47, no. 7/8, pp. 583-595, 1999.

[20] O. Kirkeby, F. Orduna, P. A. Nelson and H. Hamada, "Inverse filtering in sound reproduction," *Measurement and Control,* vol. 26, no. 9, pp. 261 - 266, November 1993.

[21] H. Tokuno, O. Kirkeby, P. A. Nelson and H. Hamada, "Inverse filter of sound reproduction systems using regularization," *IEICE Transactions on Fundamentals of Electronics, Communications and Computer Sciences,* Vols. E80-A, no. 5, pp. 809 - 820, 1997.

[22] D. Pinardi and A. Farina, "Metrics for Evaluating the Spatial Accuracy of Microphone Arrays," in *International Conference on Immersive and 3D Audio*, Bologna, 2021.

[23] S. Moreau, J. Daniel and S. Bertet, "3D sound field recording with higher order ambisonics-objective measurements and validation of spherical microphone," *120th AES Convention,* 2006.

[24] E. G. Williams, Fourier Acoustics: Sound Radiation and Nearfield Acoustical Holography, Academic Press, 1999.

[25] C. Nachbar, F. Zotter and E. Deleflie, "Ambix - A suggested Ambisonics format," *Ambisonics Simposium,* 2011.

[26] A. Farina, "Explicit formulas for High Order Ambisonics," August 2017. [Online]. Available: http://www.angelofarina.it/Aurora/HOA_explicit_formulas.htm.

[27] E. Bannai and E. Bannai, "A survey on spherical designs and algebraic combinatorics on spheres," *European Journal of Combinatorics,* vol. 30, no. 6, pp. 1392-1425, 2009.

[28] E. Bannai, "Rigid spherical t-designs and a theorem of Y. Hong," *J. Fac. Sci. Univ. Tokio,* vol. 34, pp. 485-489, 1987.

[29] E. Bannai, T. Okudab and M. Tagami, "Spherical designs of harmonic index t," *Journal of Approximation Theory,* vol. 195, pp. 1-18, 2015.

[30] E. Bannai and R. M. Damerell, "Tight spherical designs, I," *J. Math. Soc. Japan,* vol. 31, no. 1, pp. 199-207, 1979.

[31] B. Banjok, "Construction of Designs on the 2-Sphere," *Europ. J. Combinatorics,* vol. 12, pp. 377-382, 1991.

[32] X. Chen, A. Frommer and B. Lang, "Computational existence proofs for spherical t-designs," *Numerische Mathematik,* vol. 117, pp. 289-305, 2011.

[33] M. Graf and D. Potts, "On the computation of spherical designs by a new optimization approach based on fast spherical Fourier transforms," *Numerische Mathematik,* vol. 119, pp. 699-724, 2011.

[34] H. Teutsch, Modal Array Signal Processing: Principles and Applications of Acoustic Wavefield Decomposition, Springer, 2007.

[35] F. Zotter and M. Frank, Ambisonics - A Practical 3D Audio Theory for Recording, Studio Production, Sound Reinforcement, and Virtual Reality, Springer, 2019.

[36] J. W. S. Rayleigh, The Theory of Sound - Volume II, New York: Dover Publications, 1896.

[37] B. Rafely, Fundamentals of Spherical Array Processing, Springer-Verlag Berlin Heidelberg, 2015.

[38] A. Politis, "Acoustical Spherical Array Processing Library," Department of Signal Processing and Acoustics, Aalto University, Finland, 2016. [Online]. Available: http://research.spa.aalto.fi/projects/spharrayproc-lib/spharrayproc.html#59.

[39] D. Pinardi, "A Human Head Shaped Array of Microphones and Cameras for Automotive Applications," in *I3DA - International Conference on Immersive and 3D Audio*, Bologna, 2021.

D. Pinardi received the M.S. (Cum Laude) degree in mechanical engineering from University of Parma, Italy, in July 2016, with a thesis on loudspeaker modelling. In March 2020, he got the Ph.D. degree in industrial engineering with a thesis on the design of microphone, hydrophone and camera arrays for spatial audio recording.

He is a research assistant of Prof. Angelo Farina from 2016, mainly specialized in spatial audio. Topics of his interest are design of sensors arrays, simulations and auralization, applied to automotive field and underwater acoustics.